AAPS PharmSciTech (2022) 23: 205
https://doi.org/10.1208/s12249-022-02351-4

RESEARCH ARTICLE

Novel Advances in 3-D Printing Technology in Drug Delivery

Design of a Personalized Nasal Device (Matrix-Piston Nasal Device, MPD) for Drug Delivery: a 3D-Printing Application

Ioanna-Maria Menegatou[1] · Paraskevi Papakyriakopoulou[1] · Dimitrios M. Rekkas[1] · Paraskevas Dallas[1] · Georgia Valsami[1]

Received: 2 April 2022 / Accepted: 28 June 2022 / Published online: 28 July 2022

Abstract

The purpose of the current study is the development and the in vitro evaluation of a novel device for the nasal delivery of biodegradable polymeric films. The Matrix-Piston nasal Device (MPD) was designed and then printed employing Fused Deposition Modeling. Particularly, the CAD model of MPD was produced considering the human anatomical features of the nasal cavity and aiming to deliver the formulation on the olfactory region. The device consists of two independent parts constructed by different materials. For the 3D-printing process, different materials were tested to decide the most applicable for each part. More precisely, Thermoplastic Polyurethene (TPU) polymer was selected to print the matrix, while Acrylonitrile Butadiene Styrene (ABS) for the piston. Furthermore, two nasal casts were printed to be used for the assessment of the device. Namely, an hydroxypropyl-methyl cellulose-based drug-free film, containing polyethylene glycol 400 as plasticizer and methyl-β-cyclodextrin as permeation enhancer, was formed on the MPD to be tested for its ability to be detached from the device and positioned on the artificial olfactory region of the nasal cast. The deposition of the film on the targeted area of the semi-realistic nasal cast took place successfully.

Keywords Intranasal administration · 3D-printing · Nasal device · Nasal films

Introduction

Intranasal (IN) delivery is an administration route suitable for brain targeting. Such non-invasive strategies gain greater acceptance by the physicians and patients. Since 2019, three nasal products have been approved for the management of epileptic seizures (midazolam, Nayzilam®; diazepam, Valtoco®) [1, 2] and resistant depression (esketamine, Spravato®) [3].

Furthermore, a sumatriptan nasal powder (Onzetra®/Xsail®) has been approved for the acutetreatment of migraine [4], while sumatriptan nasal spray has been on the market since 1997 [5]. Neuroprotective substances and natural antioxidants can provide defense to the neural cells against neurodegenerative diseases, such as Alzheimer's and Parkinson's disease. The bioavailability of these substances is found reduced in the brain, either because of the first-pass effect, or due to their inability to cross the blood brain barrier (BBB) [6]. Nose-to-brain delivery can increase the levels of the administered drugs into the brain, bypassing the BBB and achieving therapeutic concentrations, with the potential to delay the progression of neurodegenerative diseases [7]. Moreover, the IN administration route is suitable for patients with swallowing problems, significantly improving their compliance [8]. Additionally, fewer systemic side effects are observed, along with the faster onset of action and the avoidance of the gastrointestinal degradation and the first-pass effect [9]. Last, but not least, several studies have shown increased drug bioavailability into the brain after IN administration, compared to intravenous administration [10, 11].

The nasal devices available on the market comply with the official requirements of the approved nasal sprays and powders [12, 13]. In 2003, the FDA published a guidance about in vitro tests required to prove the reproducibility and

✉ Georgia Valsami
valsami@pharm.uoa.gr

[1] Department of Pharmacy, School of Health Sciences, National and Kapodistrian University of Athens, Panepistimiopolis, 15784 Zografou, Greece

accuracy of mechanical liquid spray pumps and pressurized metered-dose inhalers (pMDIs) [14]. The variability of their performance is related to the non-reproducible deposition of the drops or particles on the olfactory region which is the target area. However, droplets produced by nebulizers are more efficiently deposited to this region, upon nasal inhalation [15]. The ease of formulation and administration of nasal liquid forms, combined with their low-cost development, has resulted in their prevalence on the market [16]. Comparative studies of sumatriptan nasal powder, with the conventional nasal spray, revealed that the IN administration of a lower dose as nasal powder resulted in earlier onset of efficacy, without causing higher than mild discomfort or abnormal taste to most of the volunteers [17]. In this context, powder formulations gain ground as they can stick on the epithelium, so that the contact time with nasal mucosa is prolonged [18]. Nevertheless, the in vivo performance of spray pumps and metered dose devices for powders' administration can be significantly different from the in vitro one, as the effectiveness of the drug delivery system is influenced by the performance of the drug delivery system and is influenced by user administration technique and the particle deposition, respectively [19].

FDM (Fused Deposition Modeling) is an extrusion-based layer by layer manufacturing method based on the melting of thermoplastic polymeric filaments [20] that form 3D objects with characteristics tailored to the purpose of their use. The available filaments allow the customization of shape, color, flexibility, density, and size of the printed objects [21]. The alteration of these factors can be applied in the design of medical devices aiming to develop personalized modes of administration depending on the needs of each patient.

In contemporary unpublished work, we tend to propose a new nasal film for nose-to-brain delivery. They are round polymeric films, with size adapted to the dimensions of the olfactory region, for the brain delivery of the acetylcholinesterase inhibitor, donepezil. These films have been evaluated in terms of in vitro and ex vivo studies and their nasal administration to mice (after the adjustment of film dimensions to the size of mice nasal cavity) showed better performance of the IN delivery compared to the oral drug delivery. In the present study, a personalized nasal device (Matrix-Piston Device, MPD) was designed to achieve the positioning of the films on the olfactory region, in order to enhance the IN absorption of drugs. Anatomical and functional characteristics of the nasal cavity were considered for the design of the MPD, employing the Autodesk Fusion 360® software. The FDM technique was adopted for the construction of this nasal device, which was then evaluated using two 3D-printed nasal casts. The device was assessed for its fit into the nostril of each nasal cast and the ability of the matrix to reach the olfactory area of the models. Moreover, the piston was considered functional when it allowed the detachment of the film from the matrix and the deposition on the target-area, after 1 to 3 rotations of the device.

Materials and Methods

Materials

The materials used for the printing of the MPD and the two nasal casts were a white PLA filament of PrimaValue® PLA series, gray and yellow TPU (Thermoplastic Polyurethene) filament of PrimaCreator® EasyPrint Flex TPU series, and a gray ABS (Acrylonitrile Butadiene Styrene) filament of PrimaSelect® ABS series, with diameter of 1.75 mm. All the materials were purchased from Prima®Creator (Sweden). Also, the white ABS and the white FiberFlex 40D filaments, with diameter of 1.75 mm, were purchased from Devil Design® and Fiberlogy®, respectively. For the preparation of the film-forming gel, methyl-β-Cyclodextrin (Me-β-CD, MW: 1310 g/mol) was bought from Fluka Chemika (Mexico City, Mexico, USA and Canada). Hydroxypropyl-methyl cellulose (HPMC, Methocel E50 premium LV, MW: 90,000 g/mol) was purchased from Colorcon (Shanghai, China). Polyethylene Glycol 400 (PEG 400) and Trypan blue solution were obtained from Sigma Chemical Company (St. Louis, MO, USA). HPLC grade water was bought from Fischer Scientific (Pittsburgh, USA).

3D-Printing Process

The MPD was designed with the Autodesk Fusion 360 software® and constructed using an FDM Creality® Ender-3 Pro printer, with printing area of 220 × 220 × 250 mm. An MK8 Extruder Driver PaT5W3 with a 1.75-mm stepper motor and 0.4-mm nozzle was employed to the printer and used for material extrusion. The printing parameters were controlled by the Creality Slicer 1.2.3® software. The PLA, ABS, TPU, and FiberFlex (thermoplastic elastomer, TPE) are generally recognized as safe (GRAS) polymers [22] and were tested as candidates for the construction of the matrix and the piston.

MPD Evaluation

The MPD evaluation was performed using a non-realistic and a semi-realistic nasal cast. The two nasal casts were constructed by materials of different flexibility and hardness allowing their distinction in non-realistic and semi-realistic. The non-realistic nasal cast was printed with rigid materials, and thus it was not able to simulate the nose pliability. On the contrary, the selection of a flexible material, such as the FiberFlex 40D filament, for the construction of the semi-realistic nasal cast allows its characterization as

"semi-realistic" as its flexibility resembles the human nose pliability. The two nasal casts were printed in the Laboratory of Biopharmaceutics & Pharmacokinetics in the Department of Pharmacy of the National and Kapodistrian University of Athens. The 3D objects were printed based on the same computer-aided design (CAD) model, obtained from the Department of Infectious Diseases of the Hospital University of Strasbourg, in France [23].

Both nasal casts consisted of two sides, corresponding to the left and right side of the face (Fig. 1). The left side offers a complete view of the inner anatomy of the nose, while the right side is closed. The two parts have been designed to be joined together forming the nasal cavity. The two sides of the non-realistic nasal cast were constructed using different materials. The left side was printed with ABS filament, while the right side was made of PLA, to assess both materials using the same nasal cast. For the semi-realistic nasal cast, the more flexible FiberFlex 40D material was employed for printing both sides, to stimulate the flexibility of the human nasal cavity. The positioning of the device inside the cavity is possible either on the left or on the right side. The MPD was assessed, using the two nasal casts, based on three evaluation criteria as follows: (a) the proper fit of the device inside the nostril, (b) the successful approach of the target area within the nasal cavity (olfactory region), and (c) the piston functionality and the ability of the device to successfully deliver the film on the target area.

Preparation of the Films

A polymer drug-free gel was prepared, to be used as a film-forming agent, according to the following method. The preparation process was based on the standard protocol of dispersion of HPMC in hot HPLC grade water (> 80 °C) and then hydration at lower temperature (< 10 °C) for 15 min [24]. PEG 400 and Me-β-CD were added as film plasticizer and permeation enhancer, respectively. The composition of the film-forming gel was 1.5% w/w HPMC E50, 1.7% w/w PEG 400, and 0.8% w/w Me-β-CD in HPLC grade water. Trypan blue 0.4% was incorporated in the film-forming gel to render the resulted film visible when its deposition on nasal cast is tested. A total of 25 μL of the film-forming gel was placed on the head of the matrix and dried for 30 min, at RT (25 °C). This volume of the gel is the maximum that can be placed on the matrix head according to the dimensions of this part of the device. The thickness of the resulted film was measured using the INSIZE Outside Micrometer (Jiangsu, China) with 0–25 mm (0.001 mm graduation) measuring range. Ten different samples were tested, and their thickness is expressed as mean ± SD.

Results and Discussion

3D-Printing of MPD

The device was composed of two distinct parts, the matrix with the base handle, and the piston, which are presented in Fig. 2. MPD was printed by the Creality Ender-3 Pro after the application of FDM printing method, employing high melting point thermoplastic polymers (Fig. 3A–C) Table(1).

Matrix

The diameters of the bottom and the upper part of the base were set to 12.7 mm and 11.3 mm, respectively. These values are close to the mean diameter of the human nostril [25]. The extension of the matrix is a tubular structure reaching a height of 3–4 cm, starting from the center of the base, with a curved head on the top where the gel-forming agent is placed and let dry to form the film (Fig. 2B-blue arrow). It targets to a distance deeper than 2–3 cm, where the nasal valve is found [26]. The olfactory region is located behind and beyond the nasal valve [18] and in a distance equal to

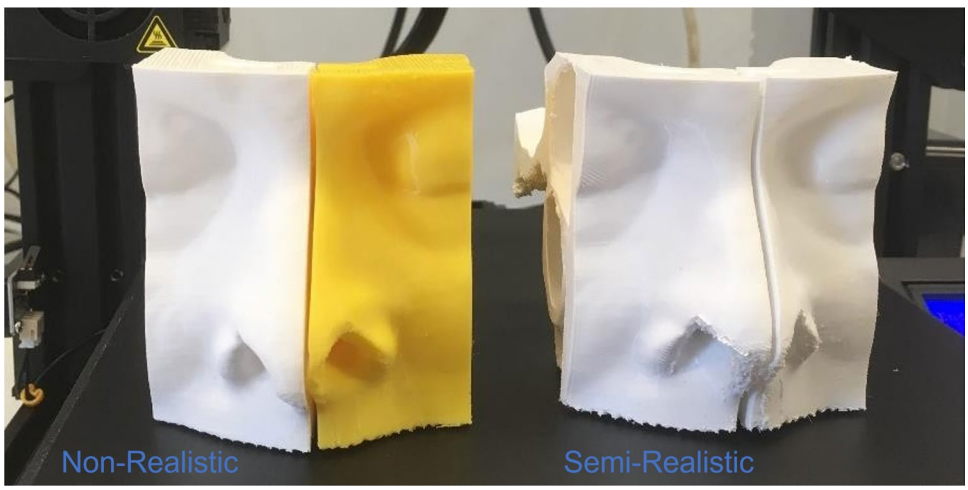

Fig. 1 Non-realistic (left) and semi-realistic (right) nasal cast

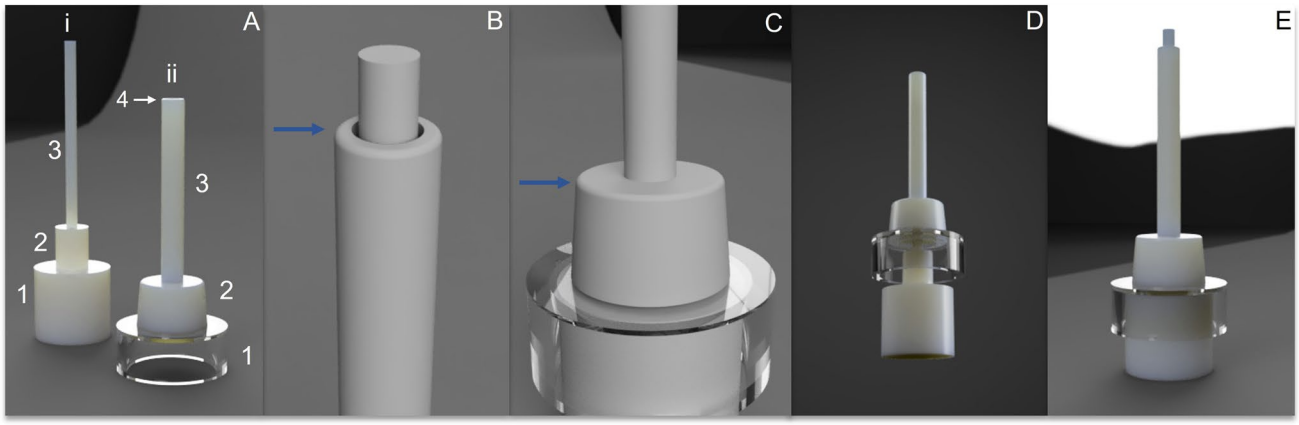

Fig. 2 **A** CAD models of (i) the matrix of MPD consisting of 1. the base handle, 2. the base, 3. the base extension, and 4. the head, where the film will be formed and (ii) the piston consisting of 1. the base handle, 2. the base, and 3. the base extension. **B** The curved head (blue arrow) of the matrix. **C** The curved base (blue arrow) of the matrix. The two parts of the MPD assembled before **D** and after **E** the film release

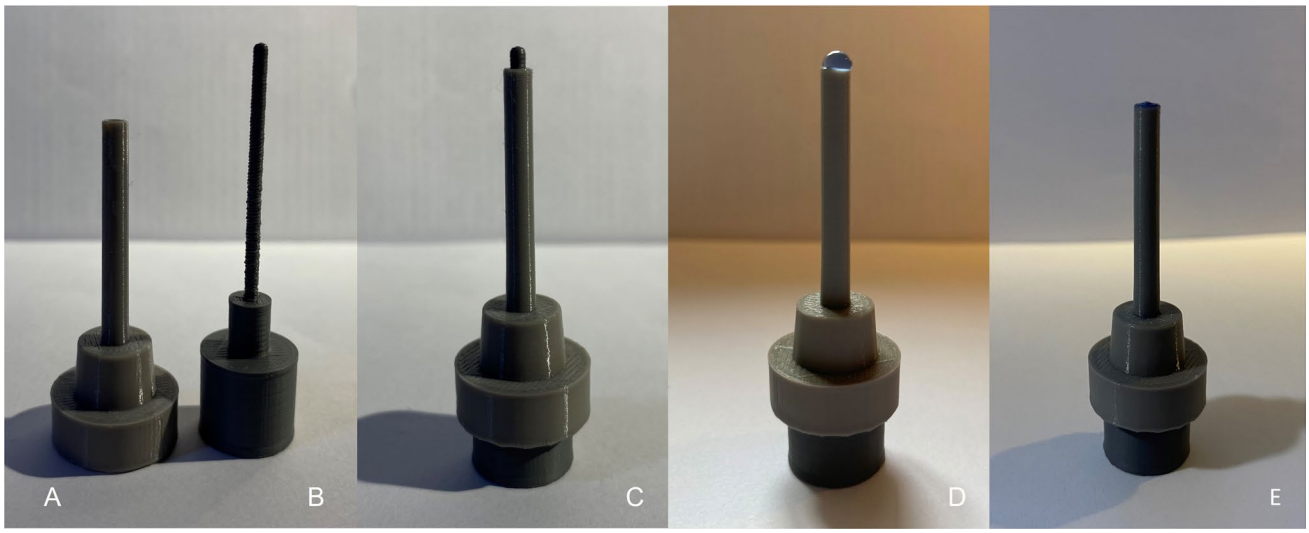

Fig. 3 **A** TPU matrix, **B** ABS piston, **C** assembled MPD, **D** the film-forming gel placed on the head of the matrix, and **E** the dry film formed on the head of the matrix

Table 1 Diameter and height characteristics of the matrix and piston

Matrix	Diameter (mm)	Height (mm)
Base handle	19.7	8.0
Base	12.7 (bottom), 11.3 (upper part)	8.0
Extension	2.7 (inner), 4.0 (external)	32.0
Head	4.0	-
Piston	Diameter (mm)	Height (mm)
Base handle	15.0	14.0
Base	6.5	8.0
Extension	2.2	36

40–42 mm from the nostril [27, 28]. For this reason, the part of the MPD placed in the nostril is equal to 44 mm. The head is attached to the top of the extension, where the gel-forming agent is placed and let dry to form the film (Fig. 3D, E). Moreover, the head and all the sides in direct contact with the nasal epithelium were curved (Fig. 2B, C-blue arrow) to avoid any discomfort or irritation during administration. PLA, TPU, and FiberFlex 40D matrices were printed with inner and external diameters of its extensions equal to 2.7 mm and 4 mm, respectively. The proper fit of the MPD inside the nasal cavity requires the parts of the base, the

extension, and the head to enter entirely inside the cavity and the base handle to protrude from the nostril. The base handle of the matrix is a non-compact cylinder, in direct contact with the base, determining the penetration depth of the device into the nasal cavity. It provides accuracy to the drug delivery on the target area and ensures the ease of device removal from the nose, after the administration. Consequently, the base of the device has a specific geometry of a non-solid cone which provides stability, while allowing the device to remain immobile inside the nasal cavity for a prolonged period. The dimensions of the device can be adjusted to that of each patient nostril to assure personalized administration. The diameter of the bases and extensions of the device, as well the length of the extension and piston proposed in this study, refers to the average characteristics of the adult human nose. Moreover, the dimensions of the nasal casts were considered to determine the size of the device. These parameters can be adjusted to the special anatomic features of each individual which differ along with the age, sex, or ethnicity. The selection of FDM technique as a proposed method for MPD printing allows the low-cost and simple construction of personalized devices, adapted to the needs of each patient. The constructed 3D objects were assessed in terms of flexibility to select the appropriate printing material for the matrix. As expected, the PLA matrix was durable but rigid, prone to cause irritation in the nasal cavity during administration, while the TPU was characterized by moderate flexibility and adequate durability. The shore hardness scale characterizes each material and enables their comparison in terms of elasticity and durability [29]. Among the three materials employed for the matrix construction, PLA has the highest shore hardness equal to 83D, while TPU and FiberFlex 40D, as more soft and elastic materials, have 95A and 40D, respectively. In the case of the FiberFlex 40D matrix, the extension's durability was low as it was deformed due to the high flexibility of the material. According to the aforementioned results, the TPU material was selected as the best material among the tested ones. Subsequently, to further optimize the flexibility and durability of the TPU matrix, three different matrices were prepared, according to the value of the fill density, which was set at four values as follows: 30%, 15%, 10%, and 0%. It was found that, as the fill density decreased, the durability decreased as well, while the flexibility increased. To assess these two parameters, the extension of each printout undergone a 90° bend. The matrix with fill density equal to 10% was successfully bended without any signs of cracking at the connection point of the extension to the base. In the case of 0% fill density, the extension came off the base, while at 30% and 15%, bending was feasible only until 40°. Consequently, the fill density equal to 10% was finally selected to ensure both the flexibility and durability of this part of the device. The printing conditions to obtain the TPU matrix of MPD are presented in Table 2. The TPU is a GRAS material [22], extensively used in medicine to produce tissue-engineered scaffolds, artificial blood vessels, implants, or prosthetics [30–32]. These polyurethane plastics are technically TPE, characterized by high elasticity (from 600 to 700% elongation to break), able to form 3D objects with soft (hardness between 60A and 55D) and flexible surface. Moreover, the biocompatibility of the TPU and the ease of its sterilization render it appropriate for the manufacturing of medical instruments and devices [33]. The tissue-like nature of this material is considered essential for the part of the MPD contacting the nasal mucosa, to avoid nose bleeding or discomfort to the patients. FiberFlex is a TPE material, presenting higher grade of flexibility and lower shore hardness [34]. Namely, in this study, the tested TPU and TPE have shore hardness equal to 95A and 40D, respectively. The geometry of the MPD extension required a degree of rigidity for its tubal structure to be formed.

Table 2 3D-printing parameters for the TPU matrix, as set to software Creality Slicer

Printing parameters	Units	Set value
Nozzle temperature	°C	215
Bed temperature	°C	70
Fill density	%	10
Print speed	mm/s	30
Travel speed	mm/s	50
Top/bottom speed	mm/s	50
Bottom layer speed	mm/s	20
Layer height	mm	0.12
Shell thickness	mm	0.8
Outer/inner shell speed	mm/s	35
Retraction speed	mm/s	80
Filament flow	%	100
Platform adhesion type	-	Raft

Piston

The piston consisted of the same parts as the matrix, without bearing a head. It was designed as a compact copy of the matrix, in smaller dimensions to fit inside the tubular extension. The height of the base handle was increased to allow the simple adjustment and removal of the piston from the matrix. The extension of the piston was designed to exit adequately from the head of the matrix and release the film formed on the matrix's head, on the targeted area of the nasal cavity. The dimensions of each part of matrix and piston are presented in Table 1. Three 3D objects were printed, each by using a different material, namely, PLA, TPU, or ABS, to determine the most appropriate one for the development of a functional piston. The FiberFlex was not tested as it does not

meet the high durability requirements. All the three pistons had an extension with a diameter of 2.2 mm and a height of 36 mm. The 3D-printing process showed that the use of PLA and ABS resulted on pistons with durable extensions, while the extension of the TPU piston was characterized by great deformation. The functionality of the piston is expressed as the ability to fit in the TPU matrix and release the film formed on its head. The PLA piston was not able to thrust the film from the TPU matrix, but could from the PLA one, while ABS piston could fit properly in the TPU matrix and had the appropriate rigidity to release the film successfully from the head. Consequently, the ABS material was selected for the construction of the piston. The printing conditions are presented in Table 3.

The ABS is a hard material with shore hardness higher than 95A, high impact strength, and minimized warping tendency [35]. Its strength is attributed to the acrylonitrile and butadiene elements, while styrene units are responsible for its toughness [36]. The ABS provided printouts with increased hardness and stability. Simultaneously, it led to negligible distortion of the piston geometry, compared with the other tested materials, such as the PLA and TPU. The piston functionality is dependable of the force that can be exerted on the film formed on the matrix head. Although PLA is more rigid, the stiffness and the rough surface of the PLA piston render the movement of its base extension into the tubal extension of the TPU matrix difficult. Accordingly, the ductility of both parts of the MPD is critical for the assemblage. The high-quality surface properties of the ABS [37] are required in this case, as the features of the PLA piston are incompatible with the TPU matrix.

The MPD was 3D-printed, based on the CAD model. The four tested materials to produce MPD have been extensively used in the development of medical devices and are FDA approved [30, 38, 39]. Grey TPU and ABS filaments were employed for the preparation of the matrix and the pistons, respectively. Then, the two parts were assembled to be used for the evaluation of film deposition in the non-realistic and semi-realistic nasal casts.

Table 3 3D-printing parameters for the ABS piston, as set to the software Creality Slicer®

Printing parameters	Units	Set value
Nozzle temperature	°C	240
Bed temperature	°C	100
Fill density	%	30
Print speed	mm/s	60
Travel speed	mm/s	80
Top/bottom speed	mm/s	80
Bottom layer speed	mm/s	20
Layer height	mm	0.12
Shell thickness	mm	0.8
Outer/inner shell speed	mm/s	35
Retraction speed	mm/s	80
Filament flow	%	100
Platform adhesion type	-	Brim

MPD Evaluation Using Nasal Casts

The MPD evaluation was performed on 3D-printed nasal casts derived by the CAD model of Sananès et al. [27]. The CAD model of the nasal cast was created by a group of scientists, to print nasal scaffolds for the training of the samplers in collection of nasopharyngeal swabs, during the COVID-19 pandemic. The nasal cast was characterized as highly realistic and anatomically accurate by 85% and 95% of the total study population ($N=40$), respectively [40].

In this study, the fit of the MPD inside the nostrils was assessed, finding that proper fit was achieved in both nasal casts, as depicted in Fig. 4. Between the two nasal casts, no anatomical differences were observed. More specifically, it was found that the base fits to the nostril, at both sides of the nasal casts, and the height of extension enables the head of the matrix to reach the targeted area. Afterwards, the film detachment from the head and deposition on the olfactory area was tested. The development of the film took place on the head of the MPD, letting the film-forming agent dry in room temperature (25 °C) for 30 min. The thickness of the formed film was equal to 45.8 ± 1.3 μm. As nasal film is a recently developing dosage form, only sparse data of the appropriate film features for nasal delivery, such as thickness, are reported in literature [41, 42]. The data of ocular films' thickness were used as reference. The maximum accepted thickness for ocular films is 90 μm [43]. Thus, the thickness of the film in this study can be considered accepted for nasal delivery, as the nasal cavity is a less fragile route of administration than the eye.

The device was introduced into the left nostril of the non-realistic and semi-realistic nasal cast. After 3 rotations of the device, the film was released successfully on the targeted area, only on the semi-realistic nasal cast (Fig. 5). The 3 rotations were required for the successful detachment of the film from the head of the matrix. The deposition of an intranasally administered formulation on the olfactory region is the first required step for drug transfer into the brain.

Limitations of the Study

Although the study effectively demonstrates the utility of a novel device for administration of nasal films, there are a few limitations associated with it. The nasal casts and the device used in this study correspond to the average dimensions of the adult nasal cavity. Moreover, the evaluation

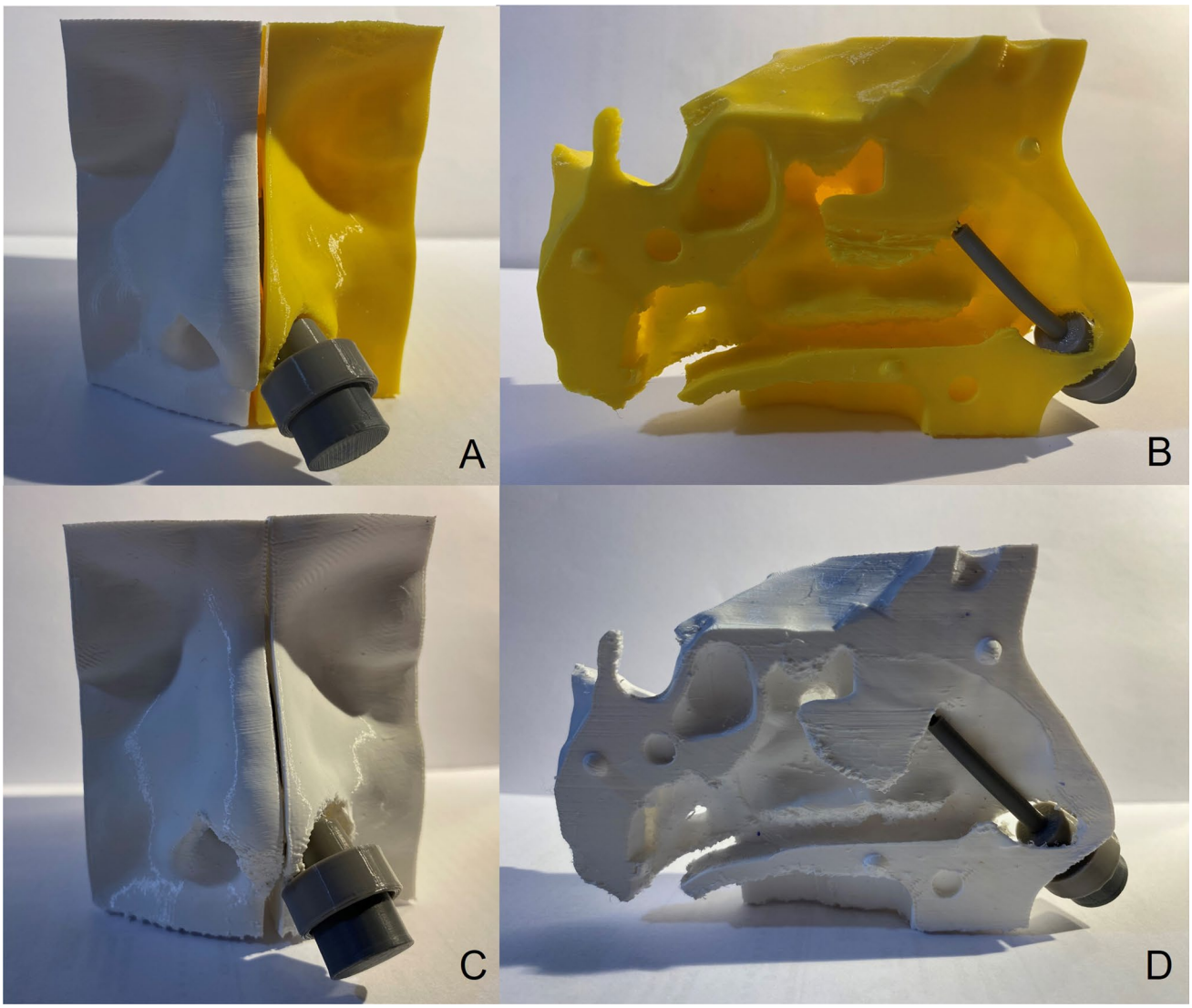

Fig. 4 MPD fit into the 3D-printed nasal casts. **A** En face non-realistic nasal cast, **B** profile left side of the non-realistic nasal cast, **C** en face semi-realistic nasal cast, **D** profile left side of the semi-realistic nasal cast

tests on the nasal casts aim to assess the deposition of the film on the target area, without considering the events that regularly take place in the nasal cavity, such as the mucociliary clearance, blood flow, congestion, and decongestion. To determine the effect of these parameters, further evaluation on healthy volunteers is required, including adult and non-adult subjects. Furthermore, the design of the device enables the administration of small size films formed by the drying of 25 μL of the film-forming agent. Low solubility drugs requiring high-dose administration cannot be delivered using this device. Despite the limitations, this study aims to develop a low-cost and easy-constructed delivery device for the recently introduced dosage form of nasal films, also proving the usefulness of 3D-printed nasal cast in its evaluation.

Conclusions

The present study introduces a realistic novel device for the personalized administration of nasal films. The evaluation of the device revealed its successful design, after being assessed in terms of film positioning on the non-realistic and semi-realistic nasal casts. The development of personalized devices for nasal delivery with 3D-printing technologies, as applied in this work, can significantly improve the effectiveness of the IN formulations. In vitro evaluation can be efficiently performed using nasal cast models; however, clinical studies on healthy volunteers are required to support the applicability of the device.

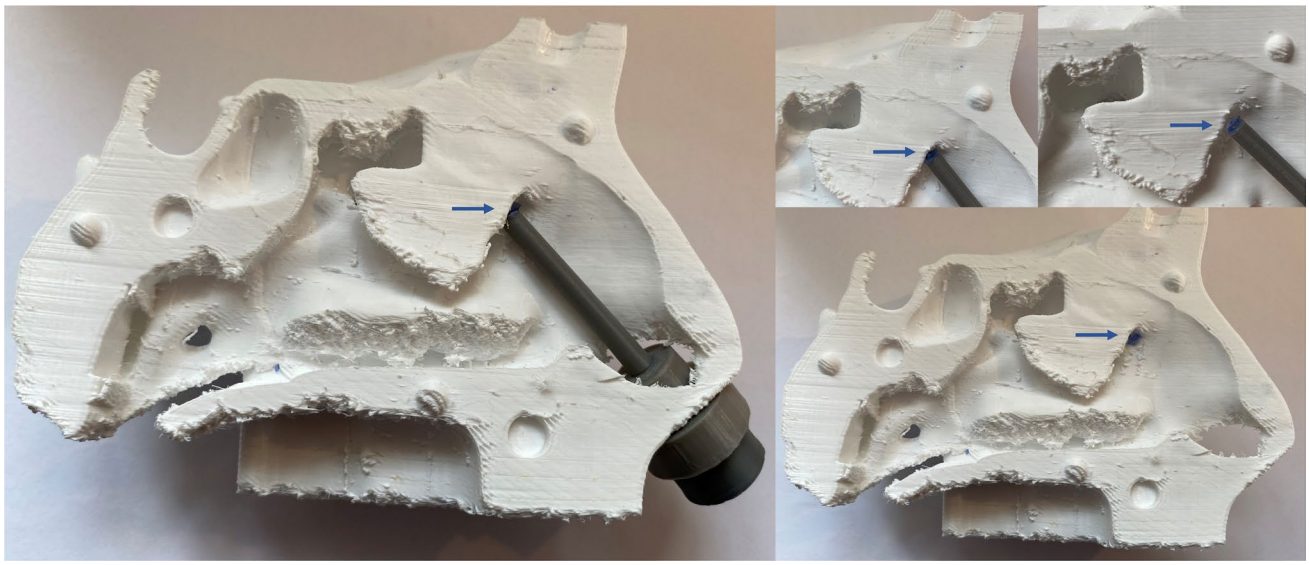

Fig. 5 Successful positioning of the nasal film (blue arrows) on the olfactory area of the semi-realistic nasal cast, using MPD

Acknowledgements The authors would like to acknowledge Ilia Papadopoulou for her contribution in manuscript editing.

Author contribution Ioanna-Maria Menegatou: process and collection of the experimental data and writing (original draft); Paraskevi Papakyriakopoulou: process and collection of the experimental data and writing (original draft); Dimitrios M. Rekkas: supervision and writing (review and editing); Paraskevas Dallas: supervision and writing (review and editing); Georgia Valsami: conceptualization, methodology, supervision, and writing (review and editing).

Declarations

Conflict of interest The authors declare no competing interests.

References

1. Spencer DC, Sinha SR, Choi EJ, Cleveland JM, King A, Meng TC, Pullman WE, Sequeira DJ, Van Ess PJ, Wheless JW. Safety and efficacy of midazolam nasal spray for the treatment of intermittent bouts of increased seizure activity in the epilepsy monitoring unit: a double-blind, randomized, placebo-controlled trial. Epilepsia. 2020;61(11):2415–25. https://doi.org/10.1111/epi.16704.
2. Segal EB, Tarquinio D, Miller I, Wheless JW, Dlugos D, Biton V, Cascino GD, Desai J, Hogan RE, Liow K, Sperling MR, Vazquez B, Cook DF, Rabinowicz AL, Carrazana E; DIAZ.001.05 Study Group. Evaluation of diazepam nasal spray in patients with epilepsy concomitantly using maintenance benzodiazepines: an interim subgroup analysis from a phase 3, long-term, open-label safety study. Epilepsia. 2021 ;62(6):1442–1450. https://doi.org/10.1111/epi.16901
3. Fedgchin M, Trivedi M, Daly EJ, Melkote R, Lane R, Lim P, Vitagliano D, Blier P, Fava M, Liebowitz M, Ravindran A, Gaillard R, Ameele HVD, Preskorn S, Manji H, Hough D, Drevets WC, Singh JB. Efficacy and safety of fixed-dose esketamine nasal spray combined with a new oral antidepressant in treatment-resistant depression: results of a randomized, double-blind, active-controlled study (TRANSFORM-1). Int J Neuropsychopharmacol. 2019;22(10):616–30. https://doi.org/10.1093/ijnp/pyz039.
4. Tepper SJ, Johnstone MR. Breath-powered sumatriptan dry nasal powder: an intranasal medication delivery system for acute treatment of migraine. Med Devices: Evid Res. 2018;11:147–56. https://doi.org/10.2147/MDER.S130900.
5. Ryan R, Elkind A, Baker CC, Mullican W, DeBussey S, Asgharnejad M. Sumatriptan nasal spray for the acute treatment of migraine. Results of two clinical studies Neurology. 1997;49(5):1225–30. https://doi.org/10.1212/wnl.49.5.1225.
6. Laffleur F, Bauer B. Progress in nasal drug delivery systems. Int J Pharm. 2021;607: 120994. https://doi.org/10.1016/j.ijpharm.2021.120994.
7. Lobaina Mato Y. Nasal route for vaccine and drug delivery: features and current opportunities. Int J Pharm. 2019; 118813. https://doi.org/10.1016/j.ijpharm.2019.118813
8. Bitter C, Suter- Zimmermanna K, Surber C. Nasal drug delivery in humans, Section II: Topical Treatment of Impaired Mucosal Membranes, Topical Applications and the Mucosa. 2011; 40; 20–35. Curr Probl Dermatol. https://doi.org/10.1159/000321044
9. Meng Q, Wang A, Hua H, Jiang Y, Wang Y, Mu H, Wu Z, Sun K. Intranasal delivery of Huperzine A to the brain using lactoferrin-conjugated N-trimethylated chitosan surface-modified PLGA nanoparticles for treatment of Alzheimer's disease. Int J Nanomedicine. 2018;13:705–18. https://doi.org/10.2147/IJN.S151474.
10. Tang S, Wang A, Yan X, Chu L, Yang X, Song Y, Sun K, Yu X, Liu R, Wu Z, Xue P. Brain-targeted intranasal delivery of dopamine with borneol and lactoferrin co-modified nanoparticles for treating Parkinson's disease. Drug Deliv. 2019;26(1):700–7. https://doi.org/10.1080/10717544.2019.1636420.
11. Hong SS, Oh KT, Choi H-G, Lim S-J. Liposomal formulations for nose-to-brain delivery: recent advances and future perspectives. Pharmaceutics. 2019;11:540. https://doi.org/10.3390/pharmaceutics11100540.
12. Pontiroli AE, Tagliabue E. Therapeutic use of intranasal glucagon: resolution of hypoglycemia. Int J Mol Sci. 2019;20(15):3646. https://doi.org/10.3390/ijms20153646.

13. No authors listed. Esketamine nasal spray (Spravato) for treatment-resistant depression. Med Lett Drugs Ther. 2019; 61(1569):54-57.
14. US FDA draft guidance for industry. Bioavailability and bioequivalence studies for nasal aerosols and nasal sprays. 2003. http://www.fda.gov/cder/guidance/index.htm. Accessed July 2012.
15. Moller W, Saba GK, Haussinger K, Becker S, Keller M, Schuschnig U. Nasally inhaled pulsating aerosols: lung, sinus and nose deposition. Rhinology. 2011;49:286–91. https://doi.org/10.4193/Rhino10.268.
16. Tiozzo Fasiolo L, Manniello MD, Tratta E, Buttini F, Rossi A, Sonvico F, Bortolotti F, Russo P, Colombo G. Opportunity and challenges of nasal powders: drug formulation and delivery. Eur J Pharm Sci. 2018;113:2–17. https://doi.org/10.1016/j.ejps.2017.09.027.
17. Silberstein S, Winner PK, McAllister PJ, et al. Early onset of efficacy and consistency of response across multiple migraine attacks from the randomized COMPASS study: AVP- 825 Breath Powered® Exhalation Delivery System (Sumatriptan Nasal Powder) vs oral sumatriptan. Headache. 2017;57(6):862–76. https://doi.org/10.1111/head.13105.
18. Khan AR, Liu M, Khan MW, Zhai G. Progress in brain targeting drug delivery system by nasal route. J Controlled Release. 2017;268:364–89. https://doi.org/10.1016/j.jconrel.2017.09.001.
19. Djupesland PG. Nasal drug delivery devices: characteristics and performance in a clinical perspective—a review. Drug Deliv Transl Res. 2012;3(1):42–62. https://doi.org/10.1007/s13346-012-0108-9.
20. Gonzalez-Macia L, Killard AJ. Screen printing and other scalable point of care (POC) biosensor processing technologies. Medical Biosensors for Point of Care (POC) Applications. 2017; 69–98. https://doi.org/10.1016/B978-0-08-100072-4.00004-6
21. Wang J, Zhang Y, Aghda NH, Pillai AR, Thakkar R, Nokhodchi A, Maniruzzaman M. Emerging 3D printing technologies for drug delivery devices: current status and future perspective. Adv Drug Deliv Rev. 2021;174:294–316. https://doi.org/10.1016/j.addr.2021.04.019.
22. Chapter 1, Subchapter B: Food for human consumption, Part 177: indirect food additives: polymers. FDA department of health and human services, Title 21, Volume 3, 21CFR177.
23. Sananès N, Lodi M, Koch A, Lecointre L, Sananès A, Lefebvre N, Debry C. 3D-printed simulator for nasopharyngeal swab collection for COVID-19. Eur Arch Otorhinolaryngol. 2021;278(7):2649–51. https://doi.org/10.1007/s00405-020-06454-1.
24. Curtis-Fisk J, Sheskey P, Balwinski K, Coppens K, Mohler C, Zhao J. Effect of formulation conditions on hypromellose performance properties in films used for capsules and tablet coatings. AAPS PharmSciTech. 2012;13(4):1170–8. https://doi.org/10.1208/s12249-012-9841-0.
25. Uzun A, Akbas H, Bilgic S, Emirzeoglu M, Bostanci O, Sahin B, Bek Y. The average values of the nasal anthropometric measurements in 108 young Turkish males. Auris Nasus Larynx. 2006;33(1):31–5. https://doi.org/10.1016/j.anl.2005.05.004.
26. Calzas C, Chevalier C. Innovative mucosal vaccine formulations against influenza A virus infections. Front Immunol. 2019;10:1605. https://doi.org/10.3389/fimmu.2019.01605.
27. Escada P. Localization and distribution of human olfactory mucosa in the nasal cavities. Acta Med Port. 2013;26(3):200–7.
28. Valtonen O, Ormiskangas J, Kivekäs I, Rantanen V, Dean M, Poe D, Järnstedt J, Lekkala J, Saarenrinne P, Rautiainen M. Three-dimensional printing of the nasal cavities for clinical experiments. Sci Rep. 2020;10:502. https://doi.org/10.1038/s41598-020-57537-2.
29. Herzberger J, Sirrine JM, Williams CB, Long TE. Polymer design for 3D printing elastomers: recent advances in structure, properties, and printing. Prog Polym Sc. 2019; 101144. https://doi.org/10.1016/j.progpolymsci.2019.101144
30. Fromstein JD, Woodhouse KA. Elastomeric biodegradable polyurethane blends for soft tissue applications. J Biomater Sci Polym Ed. 2002;13:391–406. https://doi.org/10.1163/156856202320253929.
31. Fang Z, Yonghao X, Xue G, Liujun J, Yuehao X, Yongquan G, Ai-ying Z, Zeng-guo F. Fabrication of heparinized small diameter TPU/PCL bi-layered artificial blood vessels and in vivo assessment in a rabbit carotid artery replacement model. Mater Sci Eng C. 2021;112628. https://doi.org/10.1016/j.msec.2021.112628
32. -Kucińska-Lipka J, Gubanska I, Pokrywczynska M, Cieśliński H, Filipowicz N, Drewa T, Janik H. Polyurethane porous scaffolds (PPS) for soft tissue regenerative medicine applications. Polym Bull. 2017; 1–23. https://doi.org/10.1007/s00289-017-2124-x
33. Mi HY, Jing X, Napiwocki BN, Hagerty BS, Chen G, Turng LS. Biocompatible, degradable thermoplastic polyurethane based on polycaprolactone-block-polytetrahydrofuran-block-polycaprolactone copolymers for soft tissue engineering. J Mater Chem B. 2017;5(22):4137–51. https://doi.org/10.1039/C7TB00419B.
34. Bergström J. Experimental characterization techniques. Mechanics of Solid Polymers. 2015: 19–114. https://doi.org/10.1016/B978-0-323-31150-2.00002-9
35. Khanna AS. Natural degradation on plastics and corrosion of plastics in industrial environment. Reference Module in Mater Sci Eng; 2021, https://doi.org/10.1016/B978-0-12-820352-1.00105-X
36. Dromel PC, Singh D. Biomanufacturing. 3D printing in medicine and surgery; 2021. https://doi.org/10.1016/B978-0-08-102542-0.00009-9
37. Thomas DJ. 3D printing techniques in medicine and surgery. 3D Printing in Medicine and Surgery; 2021.
38. DeStefano V, Khan S, Tabada A. Applications of PLA in modern medicine. Engineered Regeneration. 2020;1:76–87. https://doi.org/10.1016/j.engreg.2020.08.002.
39. Grady BP, Cooper SL, Robertson CG. Thermoplastic elastomers. The Science and Technology of Rubber, 2013: 591–652. https://doi.org/10.1016/B978-0-12-394584-6.00013-3
40. Lecointre L, Venkatasamy A, Wehr M, Koch A, Sananes A, Debry C, Lodi M, Sananes N. Multicentric evaluation of a 3D-printed simulator for COVID- 19 nasopharyngeal swab collection in testing centers. J Infect. 2021;83(6):709–37. https://doi.org/10.1016/j.jinf.2021.09.015.
41. Laffleur F. Nasal adhesive patches - approach for topical application for dry nasal syndrome. Int J Biol. 2018;111:493–7. https://doi.org/10.1016/j.ijbiomac.2018.01.043.
42. Shrivastava L, Schütte H, Malik P, Shrivastava R. A new class of polymeric anti-allergen nasal barrier film solution for the treatment of allergic rhinitis. J Allergy Ther. 2017;8:3. https://doi.org/10.4172/2155-6121.1000263.
43. Tighsazzadeh M, Mitchell JC, Boateng JS. Development and evaluation of performance characteristics of timolol-loaded composite ocular films as potential delivery platforms for treatment of glaucoma. Int J Pharm. 2019;566:111–25. https://doi.org/10.1016/j.ijpharm.2019.05.059.